9572 *Biochemistry* **2010,** *49,* 9572–9583
DOI: 10.1021/bi101334j

BIOCHEMISTRY
including biophysical chemistry & molecular biology
Article

CHOBIMALT: A Cholesterol-Based Detergent†

Stanley C. Howell,‡ Ritesh Mittal,‖ Lijun Huang,‖ Benjamin Travis,‖ Richard M. Breyer,§ and Charles R. Sanders*,‡

‡*Department of Biochemistry, Center for Structural Biology, and* §*Division of Nephrology, Department of Medicine, Vanderbilt University School of Medicine, Nashville, Tennessee 37232, United States, and* ‖*Anatrace-Affymetrix, 434 West Dussel Drive, Maumee, Ohio 43537, United States*

Received August 18, 2010; Revised Manuscript Received October 2, 2010

ABSTRACT: Cholesterol and its hemisuccinate and sulfate derivatives are widely used in studies of purified membrane proteins but are difficult to solubilize in aqueous solution, even in the presence of detergent micelles. Other cholesterol derivatives do not form conventional micelles and lead to viscous solutions. To address these problems, a cholesterol-based detergent, CHOBIMALT, has been synthesized and characterized. At concentrations above 3−4 μM, CHOBIMALT forms micelles without the need for elevated temperatures or sonic disruption. Diffusion and fluorescence measurements indicated that CHOBIMALT micelles are large (210 ± 30 kDa). The ability to solubilize a functional membrane protein was explored using a G-protein coupled receptor, the human kappa opioid receptor type 1 (hKOR1). While CHOBIMALT alone was not found to be effective as a surfactant for membrane extraction, when added to classical detergent micelles CHOBIMALT was observed to dramatically enhance the thermal stability of solubilized hKOR1.

The purification and biophysical characterization of integral membrane proteins (MPs)[1] usually require that MPs first be extracted out of their membrane bilayer environment, a task for which detergents are usually employed. Ideally, mild detergents allow MPs to be solubilized while preserving native-like structure and function. From numerous biophysical and biochemical studies of MPs (*2*−*4*), certain detergents are well established as tools in the study of MPs, a fact that reflects both commercial availability and affordability as well as specific properties such as effectiveness at MP extraction/solubilization of membrane proteins, ability to preserve the functional state, and the compactness and homogeneity of the protein/detergent complexes formed (*3*, *5*, *6*). There remains great interest in developing detergent systems to mimic key aspects of native membrane environments not well represented by available systems (*7*). For example, there is a need for surfactants that mimic specific lipids found in the membranes of complex organisms.

A hallmark of the lipid compositions of vertebrate membranes is the presence of cholesterol, often at concentrations in the range of 5−30 mol % of the total membrane lipid (*8*−*12*), with concentrations in microdomains approaching 50 mol % (*13*−*17*). Cholesterol plays crucial roles in modulating membrane structure, dynamics, and phase behavior (*18*−*21*) and is a major component of ordered subdomains often referred to as "lipid rafts". Many membrane proteins are believed to interact specifically with cholesterol in ways that alter their stability, function, and trafficking (*22*−*26*).

While detergents are available that mimic a number of the major classes of phospholipids found in the membranes of higher organisms, cholesterol represents a membrane component for which improved surfactant mimetics are needed. Cholesterol hemisuccinate and cholesterol sulfate are commercially available (Figure 1) but have limited solubility even in the presence of excess conventional detergent. Other cholesterol derivatives have higher solubility and have been used for cationic liposomal DNA transfection: cholesteryl-PEG_{600}, *N*-trimethylammonioethanecarbamoylcholesterol (TMAEC-CHOL), and *N*-triethylaminopropanecarbamoylcholesterol iodide (TEAPC-CHOL). However, these compounds exhibit a strong tendency to form worm-like micelles and liposomes (*27*−*29*), rather than classical micelles. Moreover, cholesteryl-PEG_{600} in not a homogeneous compound, but rather a mixture of compounds with PEG chains of varying length. The bile salts and related detergents (CHAPS and CHAPSO) exhibit favorable physical properties but cannot be regarded as true cholesterol analogues because their molecular polar/apolar topologies are very different from cholesterol, leading to modes of interactions with both membranes and proteins that are fundamentally dissimilar from cholesterol. Finally, although digitonin, the saponins, and related compounds have played roles in the history of membrane protein biophysics, they also deviate significantly in molecular topology from cholesterol such that they too cannot be considered to be true analogues.

A recent report (*1*) described the preliminary use of a novel water-soluble derivative of cholesterol, β-cholesteryl-(maltosyl-β-(1,6)-maltoside) (CHOBIMALT), in studies of the 99-residue

†This study was supported by NIH Grants RO1 GM081816 (to C.R.S.) and R43 MH081379 (to B.T.).

*To whom correspondence should be addressed. E-mail: chuck.sanders@vanderbilt.edu. Phone: 615-936-3656. Fax: 615-936-2211.

[1]Abbreviations: 8-ANS, 8-anilino-1-naphthalenesulfonic acid; β_2AR, β_2 adrenergic receptor; BzCl, benzoyl chloride; CHOBIMALT, β-cholesteryl-(maltosyl-β-(1,6)-maltoside); CHAPS, 3-[(3-cholamidopropyl)dimethylammonio]-1-propanesulfonate; CHAPSO, 3-[(3-cholamidopropyl)-dimethylammonio]-2-hydroxy-1-propanesulfonate; CHS, cholesteryl hemisuccinate; cholesteryl-PEG_{600}, cholesteryl-polyethylene glycol-600; CMC, critical micellar concentration; CSA, camphorsulfonic acid; DBU, diaza(1,3)bicyclo[5.4.0]undecane; DCM, dihloromethane; DDM, dodecyl maltopyranoside; DMF, dimethylformamide; DPC, dodecylphosphocholine; D_t, translational diffusion coefficient; GPCR, G-protein coupled receptor; hKOR1, human kappa opioid receptor type 1; MeONa, sodium methoxide; MP, integral membrane protein; NMR, nuclear magnetic resonance; LMPC, lysomyristoylphosphatidylcholine; PAGE, polyacrylamide gel electrophoresis; $PhCH(OMe)_2$, 2,2-dimethoxyethylbenzene; Py, pyridine; SDS, sodium dodecyl sulfate; TEAPC-CHOL, *N*-triethylaminopropanecarbamoylcholesterol iodide; THF, tetrahydrofuran; TM, transmembrane segment; TMAEC-CHOL, *N*-trimethylammonioethanecarbamoylcholesterol; TMSOTf, trimethylsilyl trifluoromethanesulfonate; POPC, 1-palmitoyl-2-oleoyl-*sn*-glycero-3-phosphocholine; TCA, trichloroacetic acid; TDPC, tetradecylphosphocholine.

 Published on Web 10/04/2010

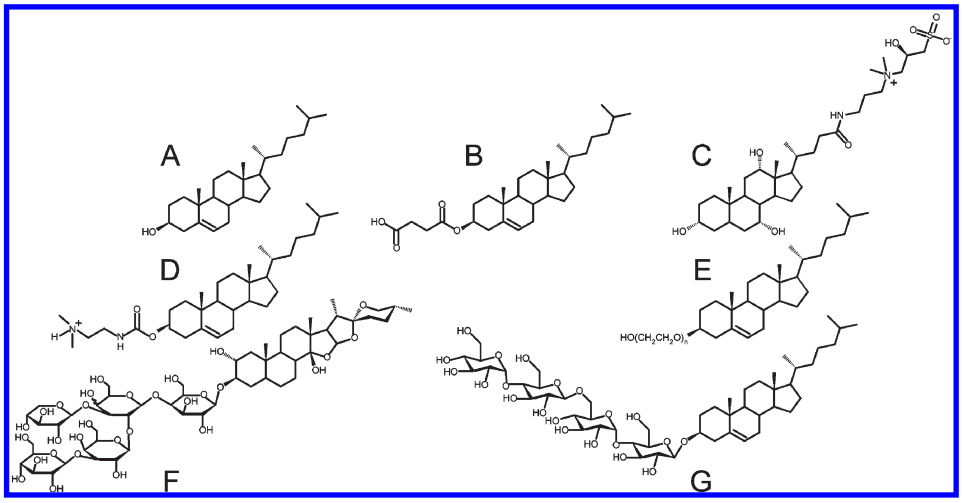

FIGURE 1: Structures of cholesterol-derived amphiphiles and related compounds: A, cholesterol; B, cholesteryl hemisuccinate (CHS); C, CHAPSO; D, DC-CHOL (TMAEC-CHOL); E, cholesteryl-PEG_{600} ($n_{average}$ 10−11); F, digitonin; G, CHOBIMALT.

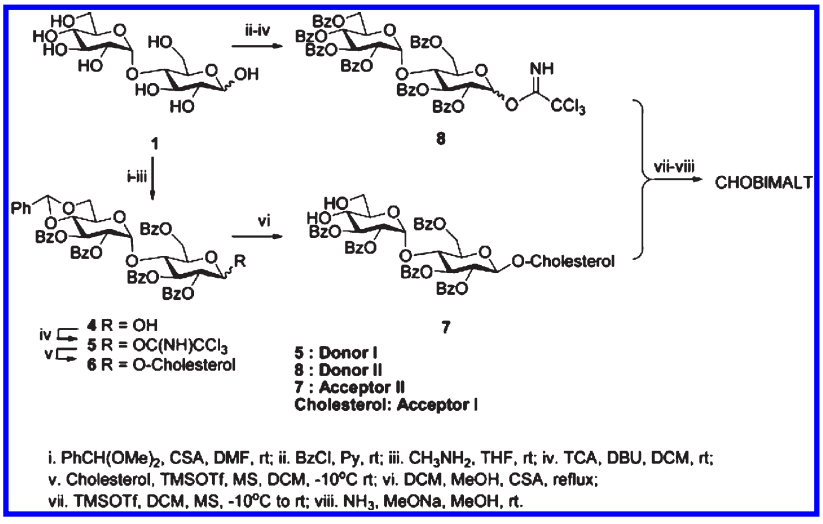

FIGURE 2: Key intermediates in the synthesis of CHOBIMALT.

C-terminal domain of the amyloid precursor protein (C99). CHOBIMALT is comprised of cholesterol that has been β-glycosylated with a β-(1,6)-linked bismaltoside. In that work, CHOBIMALT was used to demonstrate that C99 is a cholesterol binding protein, experiments that were possible only as a result of the high aqueous solubility of this compound relative to cholesterol or other available polar headgroup-derivatized compounds. Here we describe the synthesis and basic physical chemical properties of CHOBIMALT and the micelles it forms. Possible application of CHOBIMALT in biophysical studies of membrane proteins is also explored using a G-protein coupled receptor.

MATERIALS AND METHODS

Materials. Unless otherwise noted, reagents were purchased from Sigma (St. Louis, MO). 8-Anilino-1-naphthalenesulfonic acid solutions (CMC dye solution), dodecylphosphocholine (DPC), tetradecylphosphocholine (TDPC), and *n*-dodecyl β-maltoside (DDM) were purchased from Affymetrix-Anatrace (Maumee, OH). Deuterium oxide (99.9%) was purchased from Cambridge Isotope Laboratories (Andover, MA). [^{3}H]Diprenorphine was obtained from Perkin-Elmer Radiochemicals (Waltham, MA). 1-Palmitoyl-2-oleoyl-*sn*-glycero-3-phosphocholine (POPC) was obtained from Genzyme Pharmaceuticals (Cambridge, MA). TMAEC-CHOL was purchased from Avanti Polar Lipids (Alabaster, AL). Zeba Spin desalting columns (7 kDa MWCO, 0.5 mL) were purchased from Pierce/Thermo Scientific (Rockford, IL). Penta-His antibody was purchased from Qiagen (Valencia, CA). Anti-mouse IgG−alkaline phosphatase was purchased from Southern Biotech (Birmingham, AL).

Synthesis of CHOBIMALT. The synthetic route highlighting the key intermediates (donor I, **5**; donor II, **8**; and acceptor II, **7**) is summarized in Figure 2. The synthesis of donor I (**5**) was initiated by an O-4′,6′-regioselective protection of maltose (**1**). This was accomplished by utilizing a 1,3-selective camphorsulfonic acid- (CSA-) catalyzed benzylidene ring formation reaction. Subsequent global protection of all the remaining hydroxyls of the benzylidene−maltose intermediate with benzoyl chloride in pyridine provided the fully protected maltose. This intermediate was selectively hydrolyzed at the anomeric position using methylamine which was then subjected to a base- (DBU-) catalyzed reaction with trichloroacteonitrile to provide donor I (**5**) in an overall yield of ca. 50% over four steps.

Donor II (**8**) was prepared in a similar fashion when compared to donor I (**5**) by an initial global protection of all the hydroxyl groups of the maltose (**1**) with benzoyl chloride in pyridine. This fully benzoylated intermediate was selectively hydrolyzed at the

anomeric position using methylamine. This was then subjected to a base- (DBU-) catalyzed reaction with trichloroacetonitrile to provide donor II (**8**) in an overall yield of ca. 60% over three steps. Both the three- and four-step protocols to obtain donors II and I, respectively, were carried out with minimal workup, and the resultant trichloroimidates were each separated by silica gel column chromatography eluted using ethyl acetate and hexanes, and the purified molecules were analyzed and confirmed by ^{1}H NMR.

Cholesterol (acceptor I) and **5** (donor I) were then subjected to Lewis acid- (TMSOTf-) catalyzed glycosylation in DCM at reduced temperature to obtain the β-isomer (**6**) which was then purified by silica gel column chromatography and again confirmed by ^{1}H NMR. Subsequent deprotection of the benzylidene moiety with an equivalent amount of CSA in refluxing DCM−methanol provided the acceptor II (**7**) in 66% overall yield over two steps.

Donor II (**8**) and acceptor II (**7**) were then subjected to a similar Lewis acid- (TMSOTf-) catalyzed glycosylation reaction in DCM at reduced temperature to obtain the β-isomer as the major product which was then purified by silica gel column chromatography. The purified β-isomer of fully protected CHOBIMALT was then analyzed to confirm the structure by ^{1}H NMR. Global deprotection of the benzoyl groups with sodium methoxide−ammonia in methanol provided the crude target molecule. This crude material then underwent a final purification using a C18 reverse-phase column to provide the pure CHOBIMALT in an overall yield of 10% over eight linear steps. The structure of the target molecule was characterized by ^{1}H NMR and mass spectrometry. CHOBIMALT has a molecular mass of 1035 Da.

Determination of CHOMBIMALT's Critical Micelle Concentration and Micelle Size. CHOBIMALT micelles were formed by the addition of either water or D_2O (for NMR experiments) to powdered CHOBIMALT and incubation of the solution at 40 °C for 1−2 h with intermittent vortexing. In addition to optical clarity, solubilization of CHOBIMALT was confirmed by cooling to 5 °C and subjecting the solutions to ultracentrifugation (350000*g* for 30 min), after which only a negligible pellet could be detected. An initial 10 mM stock of CHOBIMALT was prepared and serially diluted to produce the additional concentrations used in the assessment of the CMC and diffusion coefficient measurements. Samples for determination of aggregation numbers by steady-state fluorescence quenching were prepared from dilution of a 10% (97 mM) stock. Dilutions were bath-sonicated at room temperature for 1 h prior to data acquisition to facilitate free detergent dissociation.

The critical micelle concentration was measured using a fluorescent probe to monitor the premicellar to micellar transition as the concentration CHOBIMALT was increased. Changes in fluorescence were observed for two series at a fixed concentration (10 μM or 250 nM) of 8-anilino-1-naphthalenesulfonic acid (8-ANS) (*30*, *31*) across a range of CHOBIMALT concentrations using a Jobin-Yvon Fluoromax-3 spectrometer. The fluorescent probe was excited at 410 nm using a 5 nm slit width, and emission was monitored by scanning at 1 nm increments from 425 to 550 nm with a 1 or 5 nm slit width for the 10 μM or 250 nM 8-ANS series, respectively. Values reported for CHOBIMALT in water are at 464 nm. Assessment of the CMC of CHOBIMALT in buffer (10 mM sodium phosphate, 100 mM NaCl, pH 7) exhibited a slight shift in the emission spectrum and was assessed at 467 nm.

Secondary assessment of the critical micellar concentration was made using the fluorescent probe pyrene. In order to effectively monitor submicromolar events, changes in pyrene fluorescence were observed using a fixed concentration of the fluorophore across a range of CHOBIMALT concentrations. Pyrene fluorescence was excited at 337 nm using a 5 nm slit width, and emission was monitored by scanning from 350 to 450 nm using a 1 nm slit width. Changes in the pyrene emission spectra were assessed by measuring the ratio observed between the first and the third vibronic bands. The ratio observed for the pyrene I_1/I_3 bands has been previously shown to be strongly dependent on the polar environment, giving rise to a distinct transition for detergents at the CMC as pyrene partitions from a polar solvent into a nonpolar micelle core. Fitting of the intensity ratios as a function of the CHOBIMALT concentration was performed using a sigmoid described by the equation (*32*):

$$\frac{I_1}{I_3} = \frac{A_1 - A_2}{1 + e^{([\text{CHOBIMALT}] - \text{CMC}_1)/\Delta}} \quad (1)$$

where A_1 and A_2 are the upper and lower limits for the sigmoid, CMC_1 is the inflection point of the sigmoidal transition, and Δ is related to the range over which the sigmoidal transition occurs. CMC is approximated by the determined CMC_1, an approach that leads to results in good agreement with CMC determined using other methods for nonionic detergents. Samples of CHOBIMALT and dodecyl maltoside were prepared by initially dissolving powdered detergent into a fresh, nitrogen-purged 1 nM pyrene solution. Samples of cholesterol were initially solubilized in absolute ethanol by warming to 80 °C with intermittent vortexing at an initial concentration of 15 mg/mL (39 mM). This solution was then diluted to 200 μM in ethanol at 80 °C before cooling to room temperature. Aliquots from this 200 μM cholesterol stock were then injected into the 1 nM pyrene solution to prepare a 1.5 μM cholesterol solution, which was further serially diluted with a 1 nM pyrene/0.75% ethanol solution to prepare the additional test solutions needed.

CHOBMIALT's aggregation number was determined using a method based on steady-state fluorescence quenching of pyrene by coumarin-153. The application of the pyrene/quencher system has previously been used to characterize the aggregation number of several detergents (*33*, *34*). In this method, loss of micelle-partitioned pyrene fluorescence occurs when coumarin-153 occupies the same micelle, allowing the relation of the observed pyrene quenching and the concentration of micelle-partitioned quencher to be correlated to the effective micelle concentration. The aggregation number then can be derived from the effective micelle concentration and the concentration of detergent above the CMC. Partitioning of coumarin-153 was assessed independently using fixed concentrations of the fluorophore across a range of CHOBIMALT concentrations (0−10%) at room temperature, using 1 and 5 μM coumarin-153, respectively. The concentration of micelle-partitioned coumarin-153 was determined from the CHOBIMALT concentration-dependent fluorescence response observed when correlating CHOBIMALT concentration to I/I_{max} for two coumarin-153 series. Coumarin-153 spectra were collected by exciting at 428 nm (1 nm slit width) and scanning from 450 to 550 nm. Spectra were compared at the maximum of the observed emission peak, centered at 508 nm. Quenching of pyrene by micelle cooccupancy with coumarin-153 was observed by changes in the emission spectra of 1 μM pyrene in 0.1% (1.0 mM) and 0.5% (4.8 mM) CHOBIMALT across a range of coumarin-153 concentrations (0−18 μM). Pyrene spectra were observed by

exciting at 337 nm (1 nm slit width) and scanning from 350 to 450 nm. Values reported are for the sharp emission peak (I_1) observed at 375 nm. The micelle effective concentration was determined by fitting of the experimental data to the expression:

$$\ln \frac{F}{F_0} = -\frac{[\text{coumarin-153}]}{N} \quad (2)$$

where F is the fluorescence intensity of pyrene observed at a given micelle-partitioned coumarin-153 concentration [coumarin-153], F_0 is the fluorescence intensity in the absence of coumarin-153, and N is the micelle concentration. The aggregation number is then equal to the micellar CHOBIMALT concentration (which is equal to the total [CHOBIMALT] − CMC) divided by the micelle concentration (N).

Aggregate size was additionally determined through the use of NMR-measured translational diffusion rates. The translational diffusion rates were measured via NMR using 150 μL samples in Shigemi tubes and a modified stimulated echo with bipolar gradients (STE-BP) pulse sequence (*35*) with a 3-19-9 water-suppression scheme (stebpgp1s191d). Data were acquired at 500 MHz using a Bruker TXI-Z cryoprobe at 20 °C using 16 linear steps from 5% to 95% maximum gradient strength, 400 ms diffusion time, 4 ms gradient pulse, and 200 μs delay between bipolar gradients. Clusters of peaks were integrated using TopSpin2.1, and the peak integral versus gradient strength data were fit by the equation(*35*):

$$I_t = I_0 e^{-D\gamma^2 g_i^2 \delta^2 (\Delta - (\delta/3) - (\tau/2))} \quad (3)$$

Here Δ is the diffusion time, δ is the length of the gradient pulse, τ is the time between bipolar gradients, g is the gradient strength, and γ is the proton gyromagnetic ratio. Initial temperature calibration was performed using the chemical shift splitting between the hydroxyl and methyl of neat methanol, commonly used to calibrate temperatures between 178 and 330 K with a 0.5 K error (*36*). Maximum gradient strength was back-calculated from the diffusion decay observed for a 150 μL sample of water acquired at 20 °C with a 10 s recycle delay. Due to the larger diffusion coefficient of water (2.025×10^{-9} m^2 s^{-1}) (*37*) the diffusion time was lowered to 150 ms, and the length of the gradient pulse was 1 ms for an equivalent pulse program without water suppression (stegp1s1d). Back-calculation from the diffusion of water gave a maximum gradient strength of 38.21 G/cm. Diffusion measurements were made for a series of CHOBIMALT concentrations ranging from 0.1% (1 mM) to 1% (10 mM). To serve as an index to correlate the observed diffusion rates to the size of the molecular ensemble, several detergents with known aggregation numbers were employed for comparison with measurements made at 0.1% (1 mM) and 1% (10 mM) CHOBIMALT: dodecyl maltopyranoside (DDM) (*38*), dodecylphosphocholine (DPC) (*39*), tetradecylphosphocholine (TDPC) (*40*), and sodium dodecyl sulfate (SDS) (*41*). All solutions of the detergent standards were prepared at 1% (w/v) concentrations in D_2O and measured with a 400 ms diffusion time, a 4 ms gradient pulse, and a 200 μs delay between bipolar gradients as described above. Spectra for 1% samples were acquired using eight scans, integrating across the aliphatic protons (0.7−1.7 ppm). To attain better signal-to-noise ratio, the number of scans for the 0.1% CHOBILMALT diffusion experiments was increased to 64. One-dimensional ^{1}H NMR spectra were acquired for the detergents at 500 MHz using 3-19-9 water suppression at 20 °C and acquired for eight scans unless otherwise indicated. The recycle delay (D1) for all experiments was 2 s.

Solubilization of Membrane Proteins by CHOBIMALT. The gene encoding the human kappa opioid receptor type 1 (hKOR1) was subcloned into a modified pET21b(+) vector (Novagen, Madison, WI) with a noncleavable C-terminal decahistidine tag and expressed in *Escherichia coli* using conditions modified from those used for the human arginine vasopressin receptor (*42*), as described below. The pET21-hKOR1 plasmid was transformed into the C43(λDE3) (Lucigen, Middleton, WI) *E. coli* strain containing the CodonPlusRP accessory plasmid (Stratagene, La Jolla, CA). Innocula from LB starter cultures were added to M9 media supplemented with cholesterol (20 mg/L), POPC (75 mg/L), and the hKOR1 antagonist, naltrexone hydrochloride (20 μM) and grown to an OD_{600} of 0.6 at 37 °C with agitation. The temperature was then reduced to 12 °C, and the cultures were allowed 1 h of thermal equilibration prior to induction with 0.5 mM isopropyl thiogalactoside. Protein expression was continued for 36 h at 12 °C with agitation, followed by cell harvesting by centrifugation. Cells were resuspended in 50 mM Tris, pH 7.4, Dounce-homogenized, and then supplemented with Sigma protease inhibitor cocktail (50 μL/1 mL of lysate), 5 mM magnesium acetate, lysozyme, DNase, and RNase. Lysis was achieved by sonication using a Fisher sonic dismembranator with a microtip probe, sonicating for 3 min with 5 s pulses and 10 s recovery delays, followed by centrifugation at 3700 rcf for 15 min. Membranes were collected from the supernatant by ultracentrifugation for 1 h at 125000*g* across a discontinuous sucrose gradient in 50 mM Tris, pH 7.4, using two sucrose layers: 30% and 60%. hKOR1-containing membranes were collected at the interface between the layers and homogenized by repeated passage through a 27 Ga needle. Bacterially expressed hKOR1 membranes prepared using this method have been shown to retain high-affinity binding and thermal properties similar to receptors expressed and purified from mammalian cells (Howell and Sanders, unpublished data). Membrane protein content in the isolated membranes was quantified using a modified Bradford assay (Coomassie Plus; Pierce, Rockford, IL) calibrated against bovine serum albumin standards. The membranes were then aliquoted into 100 μg membrane protein aliquots, adjusted to 500 μL by the addition of 50 mM Tris, pH 7.4, and pelleted by ultracentrifugation at 300000*g* for 1 h. Membrane pellets were then resuspended by repeat pipetting in 100 μL of one of the detergent solutions: 2% CHAPSO, 2% DDM, 2% CHOBIMALT, 1.5% digitonin, 1% LMPC, or 1% DPC (all buffered with 50 mM Tris, pH 8) and then incubated at 5 °C for 4 h on a rotating platform. The solution was then ultracentrifuged at 300000*g* for 1 h. The supernatant was analyzed by SDS−PAGE followed by transfer to a nitrocellulose membrane for detection with a penta-His antibody (Qiagen, Valencia, CA) and alkaline phosphatase/nitrotetrazolium blue visualization.

Characterization of Detergent/CHOBIMALT Mixed Micelles and Testing with a GPCR. Mixed micelle samples were prepared by combining solid detergent and either CHOBIMALT or cholesterol hemisuccinate and then cosolubilized in D_2O or water to a final concentration of 5% detergent/1% cholesterol analogue. Concentrated samples were bath-sonicated with gentle warming (< 50 °C) for 2 h, followed by a final dilution to 1% detergent concentration. Diffusion coefficients were determined as described above. Due to the overlap of ^{1}H NMR resonances from the detergent and CHOBIMALT in the aliphatic region, an additional assessment of the translational diffusion coefficient for the cholesterol derivative was made from an independent fit of the diffusion coefficient to additional NMR

resonances (2.2−2.8 ppm) appearing only in the mixed micelles. Differences in the two measured diffusion coefficients would be indicative of heterogeneity of the mixed micellar solution.

Samples for assessment of GPCR functionality in the mixed micelle systems were prepared by solubilizing the hKOR1-containing membrane pellets in either 1% DDM, 1% DDM/0.2% CHS, or 1% DDM/0.2% CHOBIMALT, buffered with 50 mM Tris, pH 7.4. The final concentration of membrane protein for detergent solubilization was 1.0 mg/mL in each of the detergent solutions. hKOR1-containing *E. coli* membranes were prepared as described previously for assessing the solubilization capacity of CHOBIMALT. After resuspension of the membrane pellets in detergent solution, samples were incubated at 5 °C for 4 h and then cleared of insoluble membrane by ultracentrifugation at 300000*g* for 1 h. The detergent-solubilized receptor was aliquoted into 100 μL, ~50 μg membrane protein samples (based on initial quantification of the membrane prior to extraction) and incubated for variable time periods at 30 °C. Following thermal stressing, retention of ligand binding was assessed using the hKOR1 antagonist [^{3}H]diprenorphine at 9 nM (three times the K_d observed in membrane prior to solubilization), incubated at 5 °C for 1 h. Total binding was assessed using detergent-solubilized hKOR1 with 9 nM [^{3}H]diprenorphine. Attempts to separate the detergent-solubilized receptor from the free ligand using a glass filter-based method, with or without polyethylenimine pretreatment, failed to retain the detergent-solubilized receptor. Separation of the detergent-solubilized receptor with bound ligand from free ligand was therefore achieved by passage through a Pierce Zeba desalting spin column preequilibrated in 50 mM Tris, pH 7.4, by centrifugation at 2000*g* for 1 min. For GPCRs such as hKOR1, nonspecific binding would normally be assessed by binding of the radioligand in the presence of a large excess of cold ligand. However, in these studies it was observed that addition of a modest 1 μM excess of cold ligand, either naltrexone or norbinaltophimine, resulted in the decreased retention of the free radioligand by the spin column. Therefore, to assess the nonspecific binding in the absence of an excess of cold ligand, bacterial membranes containing an alternate G-protein coupled receptor, the human β_2 adrenergic receptor (β_2AR), were employed. β_2AR-containing membranes were used to estimate the amount of nonspecific binding of [^{3}H]diprenorphine. β_2AR-containing membranes were prepared and solubilized as described above for hKOR1 following expression of β_2AR from a modified pET21-based vector containing a nonremovable C-terminal decahistidine tag. Nonspecifically bound [^{3}H]diprenorphine was isolated using the β_2AR-containing membranes and the same spin column protocol as described above. For both specific and nonspecific binding samples, counts for the bound [^{3}H]diprenorphine were measured after the addition of 3.5 mL of Perkin-Elmer Optima Gold scintillation cocktail and incubation at room temperature for 2 h on an oscillating platform. Decay counts were made on a Beckman LS6500 multipurpose scintillation counter, averaging the counts for 10 min per sample. For each time point the reported specific binding was derived by taking the difference between the total binding in hKOR1-containing membranes and nonspecific binding in β_2AR-containing membranes. The observed loss of high-affinity binding was fit to a single exponential decay:

$$I = I_0 e^{-k_i t} \quad (4)$$

where I_0 is the normalized binding observed without incubation at 30 °C, t is the time of incubation at 30 °C, and k_i is the rate of inactivation. From the fit of the data, the half-life of the receptor at 30 °C could be determined from the relation:

$$t_{1/2} = \frac{\ln(2)}{k_i} \quad (5)$$

Binding was further assessed in the mixed micelle systems by measuring the dissociation constant for [^{3}H]diprenorphine through saturation binding. Total binding was measured using detergent-solubilized hKOR1 across a range of diprenorphine concentrations (0.16−21 nM). Nonspecific binding was assessed using equivalent amounts of solubilized β_2AR membranes in the respective detergent systems across the same radioligand concentration range. Dissociation constants were derived by fitting to a single binding site model:

$$\text{specific binding} = \frac{B_{max}[\text{DPN}]}{[\text{DPN}] + K_D} \quad (6)$$

where B_{max} is the maximum binding, DPN is the concentration of the radioligand, [^{3}H]diprenorphine, and K_D is the dissociation constant.

RESULTS

Observation of a CMC-like Phase Transition for CHOBIMALT in Aqueous Solution. Powdered CHOBIMALT could be readily solubilized to at least 45% (w/v) (430 mM) in aqueous solutions with simple vortexing or agitation at 40 °C. Though micelles prepared at 5 °C were slower to initially solubilize, samples prepared at either temperature ultimately gave no visible signs of turbidity and yielded a negligible pellet after ultracentrifugation. The solubility of CHOBIMALT (> 430 mM) is 5 orders of magnitude higher than for cholesterol (4.7 μM) (*43*). Contrary to reports of CHS solubility of 10 mM (*44*), attempts to solubilize lower concentrations of CHS (neat aqueous, pH 9.0) produced solutions exhibiting turbidity and that yielded a visible pellet when subjected to modest centrifugal force (13000*g*, 5 min), even at concentrations of only 0.1 mM. Of the commercially available compounds tested, two other cholesteryl analogues, TMAEC-CHOL and cholesteryl-PEG$_{600}$, could be solubilized at concentrations greater than 10% (w/v). However, solutions containing these compounds were markedly more viscous than comparable CHOBIMALT solutions. This likely reflects the reported tendency of the TMAEC-CHOL and cholesteryl-PEG$_{600}$ to form extended rod-shaped micelles (*27*, *29*). Moreover, 1% solutions of these compounds produced a pellet or film upon ultracentrifugation (350000*g*, 30 min), whereas solutions of CHOBIMALT did not.

In light of the ease and extent to which CHOBIMALT can be brought into an aqueous solution, it was postulated that CHOBIMALT may be capable of forming conventional micelles, which could account for its greater solubility and lower viscosity relative to other cholesteryl compounds. To assess the possible micelle-like properties of this compound, several physical parameters for the water-soluble form of CHOBIMALT were measured. An attempt to determine the critical micelle concentration (CMC) was carried out using a fluorescence method that uses 8-anilino-1-naphthalenesulfonic acid (8-ANS) to measure CMC values as low as picomolar (*30*, *31*). This method is based on quenching of the fluorescence of 8-ANS in aqueous solution, whereas upon partitioning into a micelle a significant increase in fluorescence is observed. The sudden increase in the observed fluorescence allows the CMC to be evaluated as the break point between linear regions below and above the critical micellar concentration. In the case of CHOBIMALT, the typical approach of

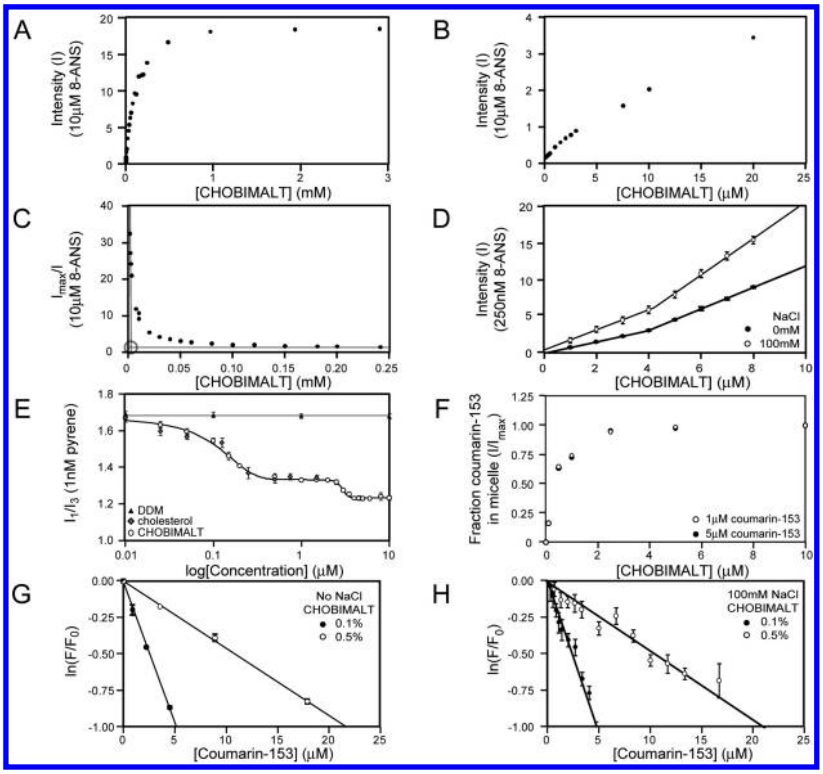

FIGURE 3: Fluorescence-based determination of the CMC and aggregation number of CHOBIMALT micelles. (A) Observed fluorescence from 10 μM 8-ANS as a function the CHOBIMALT concentration. (B) Expansion of the low [CHOBIMALT] region of (A). (C) Plots of the reciprocal of the relative fluorescence intensity from (A) versus the concentration of CHOBIMALT create a break point that leads to an estimate of CHOBIMALT's apparent critical micellar concentration (roughly 3 μM). (D) Fluorescence intensity from 250 nM 8-ANS as a function of the CHOBIMALT concentration in water only or in 10 mM sodium phosphate and 100 mM NaCl, pH 7. Apparent CMCs of 4.0 ± 0.1 and 4.2 ± 0.2 mM were derived, respectively. (E) Fluorescence from 1 nM pyrene as a function of the concentrations of CHOBIMALT, cholesterol, and DDM. In the case of CHOBIMALT the inflection points for the two sigmoidal transitions were determined to be 70 nM and 3 μM. (F) Calibration of coumarin-153 partitioning between solution and CHOBIMALT micelles using 1 and 5 μM coumarin-153. (G) Fluorescence quenching of pyrene as a function of the concentration of coumarin-153 quencher, at either 0.1% (1 mM) or 0.5% (5 mM) CHOBIMALT. From the slopes of the linear fits to these data micelle concentrations were extracted that permitted estimation of the aggregation numbers for CHOBIMALT micelles at 0.1% and 0.5% total concentrations (185 ± 35 and 222 ± 11, respectively). Samples were in pure water. (H) Same as (F) except that solutions contained 10 mM phosphate buffer, pH 7, and 100 mM NaCl. In this case aggregation numbers were determined to be 200 ± 20 at 0.1% CHOBIMALT and 228 ± 25 at 0.5%.

directly correlating detergent concentration to fluorescence intensity from 10 μM ANS was complicated by a rapid increase in fluorescence at very low (nanomolar to micromolar) detergent concentrations and the absence of a distinct linear region or a clear break point (Figure 3A,B). The absence of a clearly defined break point in fluorescence could arise either from a CMC being lower than the concentration of fluorescent probe initially tested or by 8-ANS/CHOBIMALT interactions at submicellar concentrations that reverse quenching of 8-ANS. We therefore replotted the data for Figure 3A,B using the equation:

$$[\mathrm{ANS}]_{\mathrm{F}} = [\mathrm{ANS}]_{\mathrm{total}} \left(\frac{I}{I_{\mathrm{max}}} \right) \qquad (7)$$

where I is the observed fluorescence intensity and I_{max} is the maximum fluorescence observed at high CHOBIMALT concentrations. This simple replotting, shown in Figure 3C, reveals two distinct linear regions, whose intersection corresponds to an apparent critical micellar concentration (as demonstrated for several control detergents in Supporting Information Figure S2 and Table S2). This apparent CMC was then used to carefully sample concentrations around the predicted CMC using a much lower concentration of 8-ANS (250 nM), which revealed a clear break point in the range at 4 μM (Figure 3D). While it was confirmed (see below) that the CHOBIMALT aggregates above this apparent CMC of 4 μM are micellar in nature, the fact that the fluorescence of 8-ANS increases with CHOBIMALT concentration below 4 μM suggests that CHOBIMALT is not monomeric at these "sub-CMC" concentrations but rather forms aggregates of a different nature than the micelles formed at higher concentrations.

The results described above for CHOBIMALT in pure water solutions were reproduced for solutions containing 10 mM sodium phosphate and 100 mM sodium chloride, pH 7.0, as shown in Figure 3D; the apparent CMC is 4 μM.

A second fluorescence-based method based on the use of pyrene was applied to verify the results from the 8-ANS studies summarized above and also to explore the nature of possible CHOBIMALT aggregates that may be present at concentrations below the apparent CMC. Pyrene fluorescence has previously been employed for a number of conventional detergents to aid in the assessment of micelle formation (*32*, *45*−*47*). For this purpose, the characteristic behavior of the vibronic band intensities of the pyrene emission spectrum was examined. The ratio of two of the bands, I_1 (~372−378 nm) and I_3 (~383−388 nm), was used as a probe of the polar environment of the pyrene probe. In the absence of a micelle, the pyrene is solvated by the polar solvent and gives rise to high I_1/I_3 ratio, observed in this study to be ~1.7 in water at 20 °C. In the presence of micelles, pyrene readily partitions into the micelle core where it exhibits a much lower I_1/I_3 ratio. In the assessment of pyrene fluorescence for the

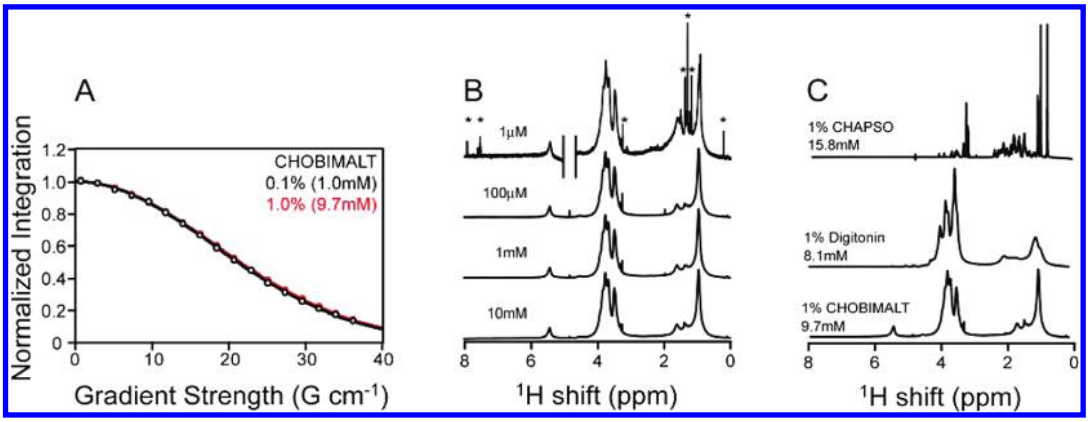

FIGURE 4: Use of NMR to assess CHOBIMALT micelle size and concentration-dependent properties. (A) Overlay of decays observed using an STE-BP sequence to measure the translational diffusion coefficient of CHOBIMALT at 1.0% (10 mM, red) and at 0.1% (1 mM, black). (B) Comparison of 1-D ^{1}H NMR spectra acquired at decreasing CHOBIMALT concentrations (from bottom to top): 10 mM (32 scans), 1 mM (512 scans), 100 μM (4096 scans), and 1 μM (4096 scans). Asterisks indicate resonances appearing at low concentration from trace contaminants. (C) Comparison of 1-D ^{1}H NMR spectra of detergent-like cholesterol analogues. The 15.8 mM CHAPSO sample represents a rapid exchange mixture between monomeric CHAPSO (estimated to be 8 mM based on its CMC) and micellar CHAPSO. Note that CHAPSO, like other bile salt-derived detergents, is believed to form very small micelles. All NMR spectra were acquired at 500 MHz at 20 °C.

common detergent dodecyl maltoside (DDM), the persistence of a high premicellar I_1/I_3 ratio (> 1.68) is observed until 100 μM, where a sudden decrease in the ratio occurs to a postmicelle ratio of < 1.15 (data not shown). Fitting of this transition gives a CMC for DDM of 0.17 ± 0.01 mM, in good agreement both with the result obtained by 8-ANS fluorescence and with literature values. Assessment of CHOBIMALT in the 1−10 μM range also reveals the distinct transition from a higher (1.33) to lower (1.23) I_1/I_3 ratio (Figure 3E). Fitting of this transition suggests an apparent CMC for CHOBIMALT of 3 μM, in agreement with the 8-ANS measurements. However, relative to the behavior of pyrene in the presence of sub-CMC concentrations of DDM (shown by the black triangles in Figure 3E), upon lowering the concentration of CHOBIMALT below CMC it is seen that there is a second sigmoidal transition that takes place before the I_1/I_3 ratio of ~1.7 is approached around 10 nM (Figure 3E). The inflection point of this transition is 70 ± 4 nM. This confirms the inference from the 8-ANS data (above) that CHOBIMALT is not monomeric as concentrations are lowered below the apparent CMC of 3−4 μM until reaching 70 nM.

Similar measurements were carried out using solubilized cholesterol. The response of the pyrene I_1/I_3 ratio to the concentration of cholesterol overlays with the response observed at nanomolar concentrations of CHOBIMALT (Figure 3E). This suggests that the aggregates formed by CHOBIMALT below its apparent CMC resemble those formed by cholesterol in the same concentration range, with both cholesterol and CHOBIMALT forming monomers in solution only below ca. 70 nM.

Confirmation of Micelle Formation and Determination of Micelle Size for CHOBIMALT. The results of the above section suggest that CHOBIMALT forms micelles at concentrations above 3−4 μM. Determination of the aggregation number was carried out using a steady-state fluorescence quenching approach. Using two fluorescent probes with overlapping emission and excitation profiles, pyrene and coumarin-153, both of which have a high propensity to partition into the micelle core, the observed quenching of the pyrene probe as the concentration of coumarin-153 is raised allows for determination of the micelle concentration. In order to calibrate the propensity of coumarin-153 to partition into the micelles, saturation of the coumarin-153 fluorescence was measured as a function of CHOBIMALT concentration (Figure 3F). Similar to 8-ANS, coumarin-153 shows a strong increase in fluorescence when partitioned into the micelle. Using 1 and 5 μM coumarin-153 and varying the CHOBIMALT concentration from 0% to 10%, the fraction of coumarin-153 partitioned from solution into the CHOBIMALT micelles could be determined by the ratio of observed fluorescence to the maximal fluorescence. No significant difference in the ratios was observed between the 1 and 5 μM coumarin-153 series, leading to determination of 16% partitioning of coumarin-153 into micelles at 1.0 mM CHOBIMALT and 64% incorporation at 4.8 mM CHOBIMALT (Figure 3F). These values were used to adjust the total concentration of coumarin-153 to the effective concentration of the quencher that is incorporated into the micelle and capable of quenching the pyrene. Next, quenching of pyrene by varying concentrations of coumarin-153 was monitored at 0.1% (1.0 mM) and 0.5% (4.8 mM) CHOBIMALT in order to determine the CHOBIMALT micelle concentration in both samples (Figure 3G). Fitting of the quenching data observed for the two series determined micelle concentrations of 4.7 μM at 0.1% (1 mM) and 19.4 μM at 0.5% (4.8 mM). Based on the previously determined CMC of CHOBIMALT of 4 μM, the aggregation number for CHOBIMALT was then determined to be 185 ± 35 and 222 ± 11, respectively, for the two concentrations tested. Similar results were obtained in samples buffered with 10 mM phosphate, pH 7.0, and containing 100 mM NaCl (Figure 3H).

Further assessment of the aggregate size of the CHOBIMALT micelles was made using NMR-based diffusion measurements (*48*, *49*). Micelle translational diffusion coefficients were extracted from a series of 1-D ^{1}H NMR experiments acquired across a range of gradient field strengths, where the integrated peak intensities are measured as a function of gradient strength to produce a decay curve, as described in Materials and Methods. In the assessment of CHOBIMALT, measurements were made at 0.1% (1 mM) and 1% (10 mM) CHOBIMALT, where it is shown in Figure 4A that nearly identical diffusion coefficients pertain (determined from these plots to be 3.4 (±0.1) × 10^{-11} m^2 s^{-1} and 3.3 (±0.1) × 10^{-11} m^2 s^{-1}, respectively). Relation of the observed translational diffusion rates for the CHOBIMALT micelles to the aggregate size of the micelle was made through comparison of the diffusion rates for other detergents for which the aggregation

number is available (Supporting Information Figure S1 and Table S1). The log of the diffusion coefficients was linear with regard to the log of the aggregate mass, as has previously been applied to establish the sizes of proteins and glucosides (*50*). Extrapolation of the linear fit for the detergent standards to the observed D_t for CHOBIMALT (Supporting Information Figure S1) suggests that CHOBIMALT micelles have an aggregate molecular mass of roughly 210 kDa. This assumes the micelles are spherical in shape, which is reasonable since this aggregate size is similar to that provided by the aggregation number orthogonally determined by the dual fluorophore quenching experiment described above.

Additional Insight on CHOBIMALT Assemblies from NMR Spectroscopy. Assessment of the 1-D ^{1}H NMR spectra of CHOBIMALT can offer insight into the nature of the transition associated with the apparent CMC observed for this compound at 3−4 μM. At concentrations well above the CMC, broad resonances arising from the dominant micelle population should be observed, which was indeed seen in the spectra shown in Figure 4B. At concentration below a true classical CMC a detergent will form monomers, which would yield a highly resolved NMR spectrum characterized by sharp peaks from the now rapidly tumbling free detergent. As seen in the top spectrum of Figure 4B, sub-CMC CHOBMALT (1 μM) does not yield sharp resonances but rather exhibits broad peaks very similar to those observed above the CMC (note that the sharp peaks present in this spectrum are from trace impurities). This indicates that below 3−4 μM CHOBIMALT populates an aggregated state, although both the 8-ANS and fluorescence measurements (Figure 3) indicate that this state is structurally distinct from the micelles seen above the apparent CMC. The pyrene fluorescence data (Figure 3E) suggest that this sub-CMC aggregate is present between 70 nM and 3 μM. Only below 70 nM does CHOBIMALT adopt a monomeric state.

Several differences can be observed in the NMR spectra of CHOBIMALT relative to CHAPSO and digitonin (Figure 4C). First, the stark difference between the bile salt derivative CHAPSO and CHOBIMALT can be seen, which reflects fundamental differences in the properties of these compounds and their assemblies. At 1% (16 mM), CHAPSO contains roughly equal populations of the free monomer and micelle-associated detergent. Moreover, bile salt-derived detergents such as CHAPSO are known to form unusually small micelles (*51*). These two factors collude to result in an NMR spectrum for a 16 mM sample that exhibits very highly resolved resonances.

The spectra of digitonin and CHOBIMALT share some similarity in the resonances arising from the sugars (3−4 ppm, Figure 4C). Notably, these resonances are quite broad, which is particularly surprising for CHOBIMALT with its normally flexible β(1→6) linkage between its two maltose groups. For both CHOBIMALT and digitonin this suggests significant conformational order in the glycoside headgroup regions of the micelles they form. There are some significant differences between CHOBIMALT and digitonin in the aliphatic region of the spectra (0−3 ppm), revealing differences that reflect structural dissimilarity and possibly different micelle properties. The peaks in the 0−3 ppm region of digitonin are quite broad, reflective of both the rigidity of the multicyclic ring system of digitonin (see Figure 1) and the moderately large size of the micelles it forms, reported to be 70−75 kDa (*52*). At first glance, the peaks in the 0−3 ppm range for CHOBIMALT appear to be significantly sharper than for digitonin, but the relatively sharp peaks arise from the alkyl tail extending from the end of the cholane ring system (see Figure 1); this tail most likely forms a molten core in the center of the CHOBIMALT micelles, a feature absent in digitonin micelles. The underlying peaks from the cholane ring system of CHOBIMALT appear to be very broad, as expected based both on low conformational mobility within the ring system and on the large size of CHOBIMALT micelles.

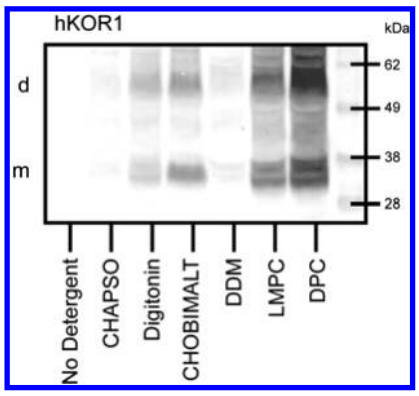

FIGURE 5: SDS−PAGE/Western blot comparison of the ability of detergents and cholesterol analogues to extract a His_{10}-tagged GPCR, hKOR1, from bacterial membranes. The following test concentrations were used: 2% CHAPSO, 1.5% digitonin, 2% CHOBIMALT, 2% DDM, 1% LMPC, and 1% DPC. Samples loaded onto this gel were extracts from membrane aliquots, each containing 15 μg of protein. Western blot detection was based on use of a mouse penta-His primary antibody and mouse IgG−alkaline phosphatase secondary antibody followed by color development mediated by alkaline phosphatase. Positions of the monomer and dimer receptor bands are indicated by the "m" and "d" on the left side.

Application of CHOBIMALT as a Detergent. To test the ability of CHOBIMALT to function as an extraction agent, we used a solubilization screen involving *E. coli* membranes into which the human kappa opioid receptor type 1 (hKOR1) was expressed with a C-terminal decahistidine tag. Membranes were extracted with a 2% CHOBIMALT solution as well as a number of other detergents commonly employed in the solubilization of membrane proteins and receptors. After extraction, any remaining membranes were removed by ultracentrifugation. The extracts were then subjected to Western blots as a readout for the effectiveness of each detergent in the solubilization of the receptor, as illustrated in Figure 5.

When extracting hKOR1 from a membrane fraction, CHOBIMALT was observed to be much less effective than DPC or LMPC at solubilizing the receptor, being comparable to digitonin, and more effective than the mild detergents CHAPSO and DDM. It was also seen that although hKOR1 solubilized using digitonin and DDM-based micelles showed some retention of high-affinity ligand binding, hKOR1 solubilized by CHOBIMALT micelles failed to produce any observable specific binding.

Impact of β-CHOBIMALT on the Size of Mixed Micelles. The potential of applying CHOBIMALT mixed micelles was explored, where a primary conventional detergent provides the protein-solubilization capacity and CHOBIMALT serves primarily to mimic cholesterol in its ability to interact with the solubilized protein or alter the micelle physical properties. This approach draws on the considerable success of stabilizing a variety of MP systems in detergent micelles by adding a cholesterol analogue (*53*−*56*). The ability to form mixed micelles between CHOBIMALT and either of two common detergents, LMPC and DDM, was assessed at the 1% DDM/0.2% CHOBIMALT (ca. 10:1 mol/mol)

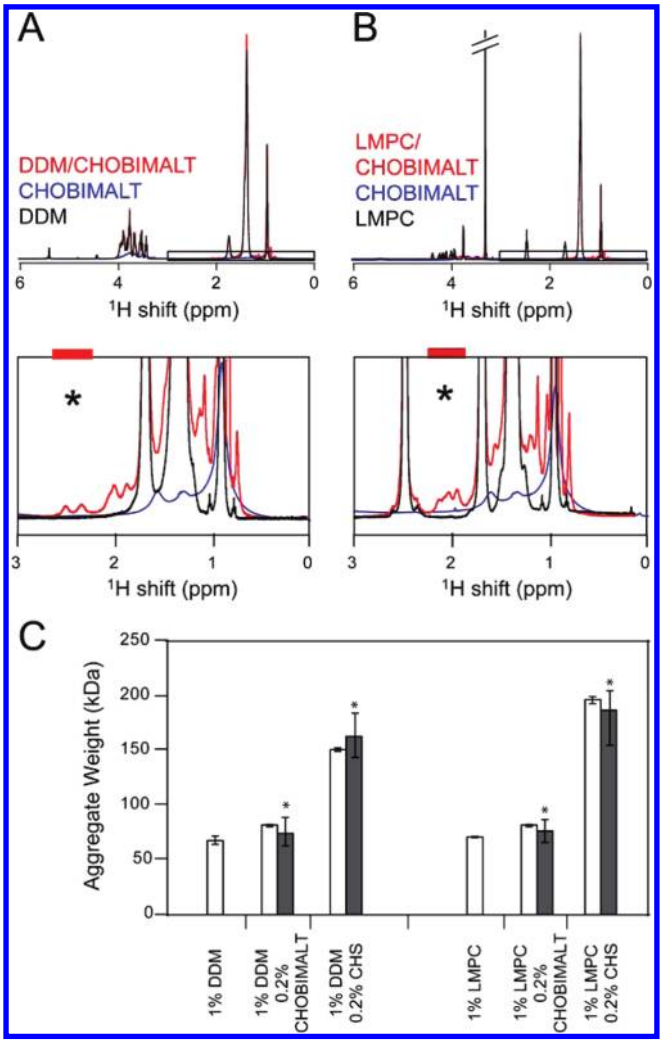

FIGURE 6: NMR assessment of the formation of mixed micelles involving detergents and cholesterol analogues. (A) Overlay of ^{1}H spectra for 1% (20 mM) DDM, 0.2% (1.9 mM) CHOBIMALT, and 1%/0.2% DDM/CHOBIMALT (ca. 10:1 mol/mol) mixed micelles. (B) Overlay of ^{1}H spectra for 1% (21 mM) LMPC, 0.2% (1.9 mM) CHOBIMALT, and 1%/0.2% LMPC/CHOBIMALT (ca. 10:1 mol/mol) mixed micelles. In both mixed micelle systems, incorporation of the cholesterol analogue into the smaller detergent micelle gives rise to the observance of resonances (1.8−2.8 ppm) not clearly seen in the spectra of the pure cholesterol analogues. Diffusion measurements were made on isolated resonances defined by the colored bars above the black asterisk, with the CHOBIMALT- or CHS-specific diffusion coefficients being compared to the results obtained by integrating over the aliphatic protons, which are dominated by signal from the detergent. (C) Influence of CHOBIMALT and CHS on the size of detergent micelles. Aggregate masses were determined from translational diffusion coefficients measured as indicated in (B), either on the aliphatic protons (white bars) or on the isolated sterol resonances (black bars).

composition. For comparison, analogous experiments using cholesterol hemisuccinate (CHS) were carried out. CHOBIMALT-containing mixed micelles rapidly produced an optically clear solution in water prior to dilution, whereas faint turbidity persisted in the concentrated solutions of the CHS mixed micelles. Dilution of the mixed micellar solutions produced clear solutions for either cholesterol analogue. To test the impact of CHOBIMALT or CHS addition on the size of the mixed micelles, NMR was used to measure the translational diffusion rates of the pure micelles and of the mixed micelles. Addition of either cholesterol analogue to the two detergent systems tested, DDM and LMPC,

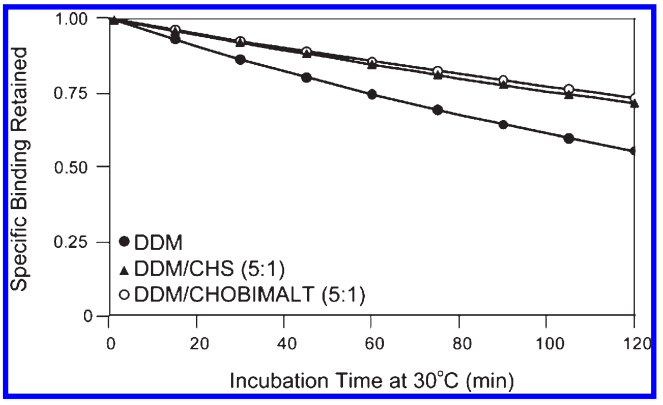

FIGURE 7: Thermal stabilization of a solubilized GPCR (hKOR1) by introducing cholesterol analogues into DDM detergent micelles: DDM (●), DDM/CHS (▲), DDM/CHOBIMALT (○). The mass ratio of 1% DDM to the cholesterol analogue was 5:1. Thermal stability was assessed at 30 °C in 50 mM Tris, pH 7.4, followed by radioligand binding at 5 °C. Specific binding of the radiolabeled antagonist [^{3}H]diprenorphine was measured as a function of incubation time in order to determine the half-life for retention of receptor function upon gradual thermal inactivation. Half-lives determined for hKOR1 are as follows: DDM, 141 ± 5 min; DDM/CHS, 247 ± 10 min; DDM/CHOBIMALT, 267 ± 8 min.

resulted in the appearance of a number of additional NMR resonances that are not present in either the free detergent or free CHOBIMALT or CHS spectra (shown in Figure 6A,B for the CHOBIMALT case). A number of resonances can be seen in the 1.8−2.8 ppm region of the spectra for each of the mixed micelles, which correspond to signals from the protons on the sterol (*57*). The fact that these additional peaks are seen only in the mixed micellar case indicates that the cholesterol analogues are associating with LMPC and DDM micelles, which are much smaller than the micelles/aggregates formed by pure CHOBIMALT or CHS. Translational diffusion rates were measured for selected resolved peaks arising exclusively from the cholesterol analogue, centered at 2.4−2.5 ppm in the DDM-based micelles and 2 ppm in the LMPC-based micelles and indicated by an asterisk on the spectra. Shown in Figure 6C are the approximate aggregate masses derived from the translational diffusion coefficients for both detergent and cholesterol analogues. The fact that for each detergent/cholesterol analogue mixture the same diffusion coefficient is obtained from both detergent and cholesterol analogue peaks indicates that these compounds form homogeneous mixed micelles. In the case of CHOBIMALT, inclusion of CHOBIMALT induces only a modest increase in micelle size for both LMPC and DDM. This contrasts with the case of CHS, which induced a dramatic increase in the size of the aggregate.

Receptor Stabilization by CHOBIMALT. The ability of CHOBIMALT to confer stability to hKOR1 solubilized by a second detergent and to preserve high-affinity ligand binding was assessed. Recombinant hKOR1 was extracted from *E. coli* membranes using 1% DDM, 1%/0.2% DDM/CHS, or 1%/0.2% DDM/CHOBIMALT. Extracts were incubated for fixed periods of time at 30 °C and then tested for the retention of specific binding of the antagonist, [^{3}H]diprenorphine. Each plot of the observed binding versus the incubation time was then fit to a simple decay function such that the half-life of the functional receptor in the detergent system could be measured, as shown in Figure 7. From the fits of the observed specific binding, the following half-lives were measured for hKOR1 in each of the micelle systems: DDM/CHOBIMALT, 267 ± 8 min; DDM/CHS, 247 ± 10 min; and DDM, 141 ± 5 min. Compared to the detergent alone, addition

of either CHOBIMALT or CHS to the DDM micelles offers a doubling of the receptor half-life observed at 30 °C. Additionally, the DDM/CHOBIMALT mixed micelle was shown to offer a slight improvement over the DDM/CHS micelle system. Measurement of the antagonist dissociation constant by a saturation binding assay revealed values similar to those observed in membrane, membrane 3.0 ± 0.1 nM, DDM 3.2 ± 0.3 nM, DDM/CHS 4.6 ± 1.1 nM, and DDM/CHOBIMALT 5.7 ± 0.2 nM, but did produce a higher B_{max} for the mixed micelle systems relative to the DDM system alone, DDM 18 ± 1 pmol/L, DDM/CHS 23 ± 1 pmol/L, and DDM/CHOBIMALT 24 ± 1 pmol/L, where the units for the B_{max} are normalized to the picomoles of receptor exhibiting high-affinity binding per liter of original culture.

DISCUSSION

Properties of CHOBIMALT and CHOBIMALT-Containing Micelles. A number of recent reports have demonstrated the value of a judicious choice of a detergent to promote the native-like structure and function of membrane proteins (*2*, *3*, *55*, *58*). However, as the MP targets for biophysical analysis continue to grow in size and complexity, the traditional complement of detergents is increasingly being found to be inadequate (*58*). CHOBIMALT was developed in order to bridge the gap between existing cholesterol-based surfactants and conventional detergents. Relative either to cholesterol or to most commercially available cholesterol analogues CHOBIMALT can be readily solubilized at high concentrations in aqueous solutions without the need for additional cosolubilizers. Preliminary studies showed that cholesterol that is β-glycosylated with only a single maltose group has low solubility (unpublished), indicating that CHOBIMALT's unique properties derive at least in part from the tetrasaccharide nature of its headgroup. It is very possible that its flexible $\beta(1\rightarrow6)$ linkage between its maltose groups is also critical to CHOBIMALT's high solubility, although this has not yet been tested.

At concentrations above 4 μM CHOBIMALT forms monodisperse micelles. With an aggregation number of roughly 200, CHOBIMALT forms 210 ± 30 kDa micelles, which are markedly larger than the micelles formed by the majority of detergents currently used for biological applications (*7*, *51*), a fact that undoubtably reflects packing constraints associated with CHOBMALT's polar headgroup and apolar "tail" domains, both of which are much larger than for most conventional detergents.

Submicromolar Behavior of CHOBIMALT. While CHOBIMALT forms micelles above 3 μM, it is unusual in that it does not appear to form monomers in the 70 nM to 3 μM concentration range. The nature of the aggregate phase formed by CHOBIMALT between 70 nM and 3 μM may be suggested from earlier reports on the behavior of soluble cholesterol, which suggest the existence of rod-like ordered aggregates at concentrations below its solubility limit of 4.7 μM (*43*). These assemblies have been postulated to involve parallel stacking of tail-to-tail dimers in which the two rings of a dimer lie along the same axis with their hydroxyls pointing outward at 180°. As the modification of cholesterol to produce CHOBIMALT is through the hydroxyls, the sugars of CHOBIMALT could be accommodated in the same aggregate morphology without disrupting the sterol−sterol interactions responsible for rod formation. The observation in this paper of an apparent CMC at 3−4 μM reflects the point of transition from these ordered aggregates to a conventional micelle. The physical−chemical basis for this transition is not clear. That this apparent CMC for CHOBIMALT is so close to the solubility limit for cholesterol supports the notion that the structural organization and forces responsible for CHOBIMALT aggregates below its apparent CMC may be very similar to those for cholesterol below its solubility limit, an interpretation strongly supported by the similarity of the pyrene fluorescence data for CHOBIMALT and cholesterol titrations, as illustrated in Figure 3E. According to this interpretation, only above 3−5 μM do the very different headgroups of cholesterol versus CHOBIMALT result in dramatically divergent solubility and aggregate properties.

We are not aware of another surfactant that resembles CHOBIMALT in terms of the concentration-dependent aggregate properties described here.

Use of CHOMBIMALT in Membrane Protein Studies. Preliminary studies employing CHOBIMALT showed that it successfully mimicked *bona fide* cholesterol in terms of its ability to undergo specific association with a protein that has a cholesterol binding site, the amyloid precursor protein (*1*). In that study CHOBIMALT was employed as a cholesterol-mimicking additive to lysomyristoylphosphatidylglycerol micelles over a range of ca. 5−50 mol %, and control experiments were carried out to verify that CHOBIMALT-induced changes in the NMR spectrum of the amyloid precursor protein reflected direct and specific protein interactions with the cholesteryl moiety of CHOBIMALT and not with the added tetraose group. In particular, changes in the NMR spectrum of the amyloid precursor protein that were induced by adding *bona fide* cholesterol to the lysolipid micelles near its solubility limit (ca. 5 mol %) were seen to be similar to the changes in the spectrum induced by a similar concentration of CHOBIMALT. In this paper the more general utility of CHOBIMALT as a reagent for MP extraction and stabilization is explored.

When used in the absence of a second detergent CHOBIMALT exhibited only modest ability to successfully solubilize the hKOR1 from the membrane, perhaps because it is too lipid-like to serve as an effective MP/lipid-solubilizing agent.

As a cosurfactant, CHOBIMALT was seen to be capable of associating with other classical detergents to form mixed micelles. While the presence of CHOBIMALT did induce a modest increase in the size of LMPC and DDM micelle assemblies, the resultant mixed micelles remained significantly smaller than the corresponding mixed micelles containing similar weight fractions of CHS. This is perhaps because in mixed micelles composed predominately of another detergent the bulky headgroup of CHOBIMALT relative to CHS serves to help minimize the size of mixed micelles by maintaining high surface curvature.

The results of this work indicate that DDM/CHOBIMALT mixed micelles confer long-term thermal stability to solubilized hKOR1 in a high-affinity ligand binding state. In this regard it is much superior to DDM alone and is comparable to DDM/CHS mixed micelles (*53*−*55*). An advantage of DDM/CHOBIMALT is that the CHOBIMALT component is much easier to solubilize than CHS. Also, the DDM/CHOBIMALT solutions were observed to be free from the tendency of DDM/CHS solutions to become turbid and produce an insoluble pellet after several days.

The roles that cholesterol plays in stabilizing native membrane proteins through modulating the properties of the bilayer and through discrete protein/cholesterol interactions continue to be unveiled (*59*). There has been strong evidence that cholesterol both enhances receptor stability and also populates specific sites on GPCRs, as explored by computational studies (*60*−*62*) and biochemical studies (*60*, *63*, *64*). Recently, the structure of the

β_2-adrenergic receptor with specifically associated cholesterol molecules has served to further illustrate roles that cholesterol may play in receptor structure (*56*). In this study we observed that CHOBIMALT is similar to CHS in that both molecules confer considerable thermal stability to micelle-solubilized hKOR1 relative to conventional micelles. That the degree of stabilization conferred by the two compounds is so similar (Figure 7) indicates that mechanism of stabilization is closely associated with the cholesteryl moiety shared by CHS and CHOBIMALT, not by their highly divergent headgroups. Nevertheless, it must be acknowledged that for both compounds the thermal stability conferred to the solubilized receptor still falls far short (ca. 10%) of the stability of the receptor in native vertebrate membranes. That the stabilization provided by CHOBIMALT and CHS is not higher very likely reflects steric occlusion of these analogues from a well-defined cholesterol binding site in hKOR1, a contention that is supported by the β_2-adrenergic receptor crystal structure, where cholesterol is packed between second and fourth transmembrane helices with only minimal space around the hydroxyl of the cholesterol. Thus, cholesterol derivatives in which its hydroxyl group has been modified are likely to be able to form optimal receptor−cholesterol interactions.

CONCLUSIONS

This work shows that CHOBIMALT exhibits high aqueous solubility and forms large micelles over a range of concentrations that is well-suited for use as a cholesterol mimic in biochemical and structural biological studies of MPs. Moreover, CHOBIMALT readily forms mixed micelles with other detergents and can be used in mixed micelles to stabilize detergent-solubilized MPs. Significant levels (up to at least 10 mol %) of CHOBIMALT in mixed micelles do not appear to trigger a major increase in micelle size above the size of the micelles formed by the conventional detergent alone. This suggests that CHOBIMALT may be particularly useful as an additive to micelles or bicelles in solution NMR studies of membrane proteins, where a premium is placed on the use of isotropic model membranes that mimic the components of native membranes while at the same time maintaining as low an aggregate molecular mass as possible.

ACKNOWLEDGMENT

We thank Drs. Wade Van Horn and Jean-Luc Popot for useful discussion and also the reviewers for helpful comments regarding an earlier version of the document.

SUPPORTING INFORMATION AVAILABLE

Figure S1 showing the NMR-measured diffusion curves for the control detergents, Figure S2 showing additional fluorescence measurements on several control detergents, Table S1 listing the control detergents used in assessing diffusion measurements, and Table S2 listing the control detergents used in assessing the fluorescence measurements. This material is available free of charge via the Internet at http://pubs.acs.org.

REFERENCES

1. Beel, A. J., Mobley, C. K., Kim, H. J., Tian, F., Hadziselimovic, A., Jap, B., Prestegard, J. H., and Sanders, C. R. (2008) Structural studies of the transmembrane C-terminal domain of the amyloid precursor protein (APP): does APP function as a cholesterol sensor? *Biochemistry 47*, 9428–9446.
2. Prive, G. G. (2007) Detergents for the stabilization and crystallization of membrane proteins. *Methods 41*, 388–397.
3. Tate, C. G. (2010) Practical considerations of membrane protein instability during purification and crystallisation. *Methods Mol. Biol. 601*, 187–203.
4. le Maire, M., Champeil, P., and Moller, J. V. (2000) Interaction of membrane proteins and lipids with solubilizing detergents. *Biochim. Biophys. Acta 1508*, 86–111.
5. Sanders, C. R., Kuhn Hoffmann, A., Gray, D. N., Keyes, M. H., and Ellis, C. D. (2004) French swimwear for membrane proteins. *ChemBioChem 5*, 423–426.
6. Silvius, J. R. (1992) Solubilization and functional reconstitution of biomembrane components. *Annu. Rev. Biophys. Biomol. Struct. 21*, 323–348.
7. Sanders, C. R., and Sonnichsen, F. (2006) Solution NMR of membrane proteins: practice and challenges. *Magn. Reson. Chem. 44* (Spec. No.), S24–S40.
8. Boesze-Battaglia, K., and Schimmel, R. (1997) Cell membrane lipid composition and distribution: implications for cell function and lessons learned from photoreceptors and platelets. *J. Exp. Biol. 200*, 2927–2936.
9. Nelson, G. J. (1967) Composition of neutral lipids from erythrocytes of common mammals. *J. Lipid Res. 8*, 374–379.
10. Gottfried, E. L. (1967) Lipids of human leukocytes: relation to celltype. *J. Lipid Res. 8*, 321–327.
11. Cheng, B., and Kimura, T. (1983) The distribution of cholesterol and phospholipid composition in submitochondrial membranes from bovine adrenal cortex: fundamental studies of steroidogenic mitochondria. *Lipids 18*, 577–584.
12. Guidotti, G. (1972) The composition of biological membranes. *Arch. Intern. Med. 129*, 194–201.
13. Brown, D. A., and Rose, J. K. (1992) Sorting of GPI-anchored proteins to glycolipid-enriched membrane subdomains during transport to the apical cell surface. *Cell 68*, 533–544.
14. Koumanov, K. S., Tessier, C., Momchilova, A. B., Rainteau, D., Wolf, C., and Quinn, P. J. (2005) Comparative lipid analysis and structure of detergent-resistant membrane raft fractions isolated from human and ruminant erythrocytes. *Arch. Biochem. Biophys. 434*, 150–158.
15. Brugger, B., Graham, C., Leibrecht, I., Mombelli, E., Jen, A., Wieland, F., and Morris, R. (2004) The membrane domains occupied by glycosylphosphatidylinositol-anchored prion protein and Thy-1 differ in lipid composition. *J. Biol. Chem. 279*, 7530–7536.
16. Rog, T., Pasenkiewicz-Gierula, M., Vattulainen, I., and Karttunen, M. (2009) Ordering effects of cholesterol and its analogs. *Biochim. Biophys. Acta 1788*, 97–121.
17. Pike, L. J., Han, X., Chung, K. N., and Gross, R. W. (2002) Lipid rafts are enriched in arachidonic acid and plasmenylethanolamine and their composition is independent of caveolin-1 expression: a quantitative electrospray ionization/mass spectrometric analysis. *Biochemistry 41*, 2075–2088.
18. Ramstedt, B., and Slotte, J. P. (2006) Sphingolipids and the formation of sterol-enriched ordered membrane domains. *Biochim. Biophys. Acta 1758*, 1945–1956.
19. Subczynski, W. K., and Wisniewska, A. (2000) Physical properties of lipid bilayer membranes: relevance to membrane biological functions. *Acta Biochim. Pol. 47*, 613–625.
20. Shimoyama, Y., Eriksson, L. E., and Ehrenberg, A. (1978) Molecular motion and order in oriented lipid multibilayer membranes evaluated by simulations of spin label ESR spectra. Effects of temperature, cholesterol and magnetic field. *Biochim. Biophys. Acta 508*, 213–235.
21. Oldfield, E., Meadows, M., Rice, D., and Jacobs, R. (1978) Spectroscopic studies of specifically deuterium labeled membrane systems. Nuclear magnetic resonance investigation of the effects of cholesterol in model systems. *Biochemistry 17*, 2727–2740.
22. Lingwood, D., and Simons, K. (2010) Lipid rafts as a membrane-organizing principle. *Science 327*, 46–50.
23. Lingwood, D., Kaiser, H. J., Levental, I., and Simons, K. (2009) Lipid rafts as functional heterogeneity in cell membranes. *Biochem. Soc. Trans. 37*, 955–960.
24. Rietveld, A., and Simons, K. (1998) The differential miscibility of lipids as the basis for the formation of functional membrane rafts. *Biochim. Biophys. Acta 1376*, 467–479.
25. Foster, L. J., and Chan, Q. W. (2007) Lipid raft proteomics: more than just detergent-resistant membranes. *Subcell. Biochem. 43*, 35–47.
26. Sengupta, P., Baird, B., and Holowka, D. (2007) Lipid rafts, fluid/fluid phase separation, and their relevance to plasma membrane structure and function. *Semin. Cell Dev. Biol. 18*, 583–590.
27. Wu, C. M., Liou, W., Chen, H. L., Lin, T. L., and Jeng, U. S. (2004) Self-assembled structure of the binary complex of DNA with cationic lipid. *Macromolecules 37*, 4974–4980.
28. Briane, D., Lesage, D., Cao, A., Coudert, R., Lievre, N., Salzmann, J. L., and Taillandier, E. (2002) Cellular pathway of plasmids

vectorized by cholesterol-based cationic liposomes. *J. Histochem. Cytochem. 50*, 983–991.
29. Harris, J. R. (2008) Cholesterol binding to amyloid-beta fibrils: a TEM study. *Micron 39*, 1192–1196.
30. Birdi, K. S., Krag, T., and Klausen, J. (1977) Determination of critical micelle concentration of anionic micellar systems by anilinonaphthalenesulfonate (Ans) in aqueous solutions. *J. Colloid Interface Sci. 62*, 562–563.
31. De Vendittis, E., Palumbo, G., Parlato, G., and Bocchini, V. (1981) A fluorimetric method for the estimation of the critical micelle concentration of surfactants. *Anal. Biochem. 115*, 278–286.
32. Aguiar, J., Carpena, P., Molina-Bolivar, J. A., and Ruiz, C. C. (2003) On the determination of the critical micelle concentration by the pyrene 1:3 ratio method. *J. Colloid Interface Sci. 258*, 116–122.
33. Turro, N. J., and Yekta, A. (1978) Luminescent probes for detergent solutions—simple procedure for determination of mean aggregation number of micelles. *J. Am. Chem. Soc. 100*, 5951–5952.
34. Tummino, P. J., and Gafni, A. (1993) Determination of the aggregation number of detergent micelles using steady-state fluorescence quenching. *Biophys. J. 64*, 1580–1587.
35. Wu, D. H., Chen, A. D., and Johnson, C. S. (1995) An improved diffusion-ordered spectroscopy experiment incorporating bipolar-gradient pulses. *J. Magn. Reson., Ser. A 115*, 260–264.
36. Ammann, C., Meier, M., and Merbach, A. E. (1982) A simple multinuclear NMR thermometer. *J. Magn. Reson., Ser. A 46*, 319–321.
37. Holz, M., Heil, S. R., and Sacco, A. (2000) Temperature-dependent self-diffusion coefficients of water and six selected molecular liquids for calibration in accurate ^{1}H NMR PFG measurements. *Phys. Chem. Chem. Phys. 2*, 4740–4742.
38. Tiefenbach, K. J., Durchschlag, H., and Jaenicke, R. (1999) Spectroscopic and hydrodynamic investigations of nonionic and zwitterionic detergents. *Prog. Colloid Polym. Sci. 113*, 135–141.
39. Arora, A., and Tamm, L. K. (2001) Biophysical approaches to membrane protein structure determination. *Curr. Opin. Struct. Biol. 11*, 540–547.
40. Strop, P., and Brunger, A. T. (2005) Refractive index-based determination of detergent concentration and its application to the study of membrane proteins. *Protein Sci. 14*, 2207–2211.
41. Bales, B. L., Messina, L., Vidal, A., Peric, M., and Nascimento, O. R. (1998) Precision relative aggregation number determinations of SDS micelles using a spin probe. A model of micelle surface hydration. *J. Phys. Chem. B 102*, 10347–10358.
42. Tian, C., Breyer, R. M., Kim, H. J., Karra, M. D., Friedman, D. B., Karpay, A., and Sanders, C. R. (2005) Solution NMR spectroscopy of the human vasopressin V2 receptor, a G protein-coupled receptor. *J. Am. Chem. Soc. 127*, 8010–8011.
43. Castanho, M. A., Brown, W., and Prieto, M. J. (1992) Rod-like cholesterol micelles in aqueous solution studied using polarized and depolarized dynamic light scattering. *Biophys. J. 63*, 1455–1461.
44. Klein, B., Kleinman, N. B., and Foreman, J. A. (1974) Preparation and evaluation of a water-soluble cholesterol standard. *Clin. Chem. 20*, 482–485.
45. Zana, R., and Guveli, D. (1985) Fluorescence probing study of the association of bile salts in aqueous solutions. *J. Phys. Chem. 89*, 1687–1690.
46. Ndou, T. T., and Vonwandruszka, R. (1990) Pyrene fluorescence in premicellar solutions—the effects of solvents and temperature. *J. Lumin. 46*, 33–38.
47. Kalyanasundaram, K., and Thomas, J. K. (1977) Environmental effects on vibronic band intensities in pyrene monomer fluorescence and their application in studies of micellar systems. *J. Am. Chem. Soc. 99*, 2039–2044.
48. Asakawa, T., Imae, T., Ikeda, S., Miyagishi, S., and Nishida, M. (1991) H-1-NMR translational diffusion study for mixed micelles of fluorocarbon and hydrocarbon surfactants. *Langmuir 7*, 262–266.
49. Cui, X., Mao, S., Liu, M., Yuan, H., and Du, Y. (2008) Mechanism of surfactant micelle formation. *Langmuir 24*, 10771–10775.
50. Groves, P., Rasmussen, M. O., Molero, M. D., Samain, E., Canada, F. J., Driguez, H., and Jimenez-Barbero, J. (2004) Diffusion ordered spectroscopy as a complement to size exclusion chromatography in oligosaccharide analysis. *Glycobiology 14*, 451–456.
51. Lipfert, J., Columbus, L., Chu, V. B., Lesley, S. A., and Doniach, S. (2007) Size and shape of detergent micelles determined by small-angle X-ray scattering. *J. Phys. Chem. B 111*, 12427–12438.
52. Smith, E. L., and Pickels, E. G. (1940) Micelle formation in aqueous solutions of digitonin. *Proc. Natl. Acad. Sci. U.S.A. 26*, 272–277.
53. Tucker, J., and Grisshammer, R. (1996) Purification of a rat neurotensin receptor expressed in *Escherichia coli*. *Biochem. J. 317* (Part 3), 891–899.
54. Weiss, H. M., and Grisshammer, R. (2002) Purification and characterization of the human adenosine A(2a) receptor functionally expressed in *Escherichia coli*. *Eur. J. Biochem. 269*, 82–92.
55. Allen, S. J., Ribeiro, S., Horuk, R., and Handel, T. M. (2009) Expression, purification and in vitro functional reconstitution of the chemokine receptor CCR1. *Protein Expression Purif. 66*, 73–81.
56. Hanson, M. A., Cherezov, V., Griffith, M. T., Roth, C. B., Jaakola, V. P., Chien, E. Y., Velasquez, J., Kuhn, P., and Stevens, R. C. (2008) A specific cholesterol binding site is established by the 2.8 Å structure of the human beta2-adrenergic receptor. *Structure 16*, 897–905.
57. Soubias, O., Jolibois, F., Reat, V., and Milon, A. (2004) Understanding sterol-membrane interactions, part II: complete ^{1}H and ^{13}C assignments by solid-state NMR spectroscopy and determination of the hydrogen-bonding partners of cholesterol in a lipid bilayer. *Chemistry 10*, 6005–6014.
58. Poget, S. F., and Girvin, M. E. (2007) Solution NMR of membrane proteins in bilayer mimics: small is beautiful, but sometimes bigger is better. *Biochim. Biophys. Acta 1768*, 3098–3106.
59. Opekarova, M., and Tanner, W. (2003) Specific lipid requirements of membrane proteins—a putative bottleneck in heterologous expression. *Biochim. Biophys. Acta 1610*, 11–22.
60. Lyman, E., Higgs, C., Kim, B., Lupyan, D., Shelley, J. C., Farid, R., and Voth, G. A. (2009) A role for a specific cholesterol interaction in stabilizing the Apo configuration of the human A(2A) adenosine receptor. *Structure 17*, 1660–1668.
61. Paila, Y. D., Tiwari, S., and Chattopadhyay, A. (2009) Are specific nonannular cholesterol binding sites present in G-protein coupled receptors? *Biochim. Biophys. Acta 1788*, 295–302.
62. Khelashvili, G., Grossfield, A., Feller, S. E., Pitman, M. C., and Weinstein, H. (2009) Structural and dynamic effects of cholesterol at preferred sites of interaction with rhodopsin identified from microsecond length molecular dynamics simulations. *Proteins 76*, 403–417.
63. Gimpl, G., and Fahrenholz, F. (2002) Cholesterol as stabilizer of the oxytocin receptor. *Biochim. Biophys. Acta 1564*, 384–392.
64. Ruprecht, J. J., Mielke, T., Vogel, R., Villa, C., and Schertler, G. F. (2004) Electron crystallography reveals the structure of metarhodopsin I. *EMBO J. 23*, 3609–3620.